Theoretical Study of Oxygen Adsorption on Pure Au_{n+1}^+ and Doped MAu_n^+ Cationic Gold Clusters for M = Ti, Fe and $n = 3-7$

M. Begoña Torres,[†] Eva M. Fernández,[‡] and Luis C. Balbás*[,§]

Departamento de Matemáticas y Computación, Universidad de Burgos, E-09006 Burgos, Spain, Center for Atomic-Scale Material Design, Department of Physics, Technical University of Denmark, DK-2800 Lyngby, Denmark, and Departamento de Física Teórica, Atómica y Óptica, Universidad de Valladolid, E-47011 Valladolid, Spain

Received: January 10, 2008; Revised Manuscript Received: April 18, 2008

A comparative study of the adsorption of an O_2 molecule on pure Au_{n+1}^+ and doped MAu_n^+ cationic gold clusters for $n = 3-7$ and M = Ti, Fe is presented. The simultaneous adsorption of two oxygen atoms also was studied. This work was performed by means of first principles calculations based on norm-conserving pseudo-potentials and numerical basis sets. For pure Au_4^+, Au_6^+, and Au_7^+ clusters, the O_2 molecule is adsorbed preferably on top of low coordinated Au atoms, with an adsorption energy smaller than 0.5 eV. Instead, for Au_5^+ and Au_8^+, bridge adsorption sites are preferred with adsorption energies of 0.56 and 0.69 eV, respectively. The ground-state geometry of Au_n^+ is almost unperturbed after O_2 adsorption. The electronic charge flows towards O_2 when the molecule is adsorbed in bridge positions and towards the gold cluster when O_2 is adsorbed on top of Au atoms, and both the adsorption energy and the O−O bond length of adsorbed oxygen increase when the amount of electronic charge on O_2 increases. On the other hand, we studied the adsorption of an O_2 molecule on doped MAu_n^+ clusters, leading to the formation of $(MAu_nO_2^+)_{ad}$ complexes with different equilibrium configurations. The highest adsorption energy was obtained when both atoms of O_2 bind on top of the M impurity, and it is larger for Ti doped clusters than for Fe doped clusters, showing an odd−even effect trend with size n, which is opposite for Ti as compared to Fe complexes. For those adsorption configurations of $(MAu_nO_2^+)_{ad}$ involving only Au sites, the adsorption energy is similar to or smaller than that for similar configurations of $Au_{n+1}O_2^+$ complexes. However, the highest adsorption energy of $(MAu_nO_2^+)_{ad}$ is higher than that for $(Au_{n+1}O_2^+)_{ad}$ by a factor of ∼4.0 (1.2) for M = Ti (M = Fe). The trends with size n are rationalized in terms of O−O and O−M bond distances, as well as charge transfer between oxygen and cluster substrates. The spin multiplicity of those $(MAu_nO_2^+)_{ad}$ complexes with the highest O_2 adsorption energy is a maximum (minimum) for M = Fe (Ti), corresponding to parallel (anti-parallel) spin coupling of MAu_n^+ clusters and O_2 molecules. Finally, we obtained the minimum energy equilibrium structure of complexes $(Au_nO_2^+)_{dis}$ and $(MAu_nO_2^+)_{dis}$ containing two separated O atoms bonded at different sites of Au_n^+ and MAu_n^+ clusters, respectively. For $(MAu_nO_2^+)_{dis}$, the equilibrium configuration with the highest adsorption energy is stable against separation in MAu_n^+ and O_2 fragments, respectively. Instead, for $(Au_nO_2^+)_{dis}$, only the complex $n = 6$ is stable against separation in Au_n^+ and O_2 fragments. The maximum separation energy of $(MAu_nO_2^+)_{dis}$ is higher than the O_2 adsorption energy of $(MAu_nO_2^+)_{ad}$ complexes by factors of ∼1.6 (2.5), 1.6 (1.7), 1.5 (2.4), 1.5 (1.3), and 1.6 (1.8) for M = Ti (Fe) complexes in the range $n = 3-7$, respectively.

Introduction

It has been shown that CO and O_2 are chemisorption promoters to each other, naturally leading to cooperative adsorption on Au clusters[1] and Au atoms.[2] As a matter of fact, the binding energy and activation of molecular oxygen by gold clusters, which are necessary steps in the CO oxidation process,[3] depend strongly on the size and state of the charge of the cluster. Thus, Cox and coworkers[4] determined experimentally several years ago that only the Au_n^- anions with even numbers of atoms, as well as the Au_{10}^+ cation, are active towards O_2. Many calculations have been performed to determine adsorption energies of molecular oxygen on gas phase anionic[5–11] and neutral[11–14] gold clusters, but very few calculations are concerned with cationic gold clusters.[15–18] For neutral clusters, Barton and Podkolzin[13]found very weak interactions between O_2 and Au_{55} but substantial bonding with Au_{13} and Au_4. Luo et al.[11]studied two isomers of Au_{24} and Au_{24}^+ and concluded that oxygen adsorption was dependent on particle shape and coordination number of the interacting gold atoms. More recently, Barrio et al.[14]found that the reactivity of neutral Au_4, Au_5, Au_{14}, Au_{25}, and Au_{29} clusters towards O_2 depends on the type of uncoordinated sites exposed, ensemble effects, and fluxionallity of the metal nanoparticles.

On the other hand, it has been shown by a combined experimental and theoretical study[19] that Au_3Sr reacts with O_2 and CO but that Au_4 does not, when these clusters are supported on well-characterized MgO (100) thin films. In another recent density functional theory (DFT) study,[20] it was shown that the presence of a platinum atom on top of a gold nanopyramid increases the adsorption of oxygen. In this study, we focused on the activity towards oxygen of pure, Au_{n+1}^+, and doped

* Corresponding author. Tel.: +34 983 423144; fax: +34 983 423013; e-mail: balbas@fta.uva.es.
† Universidad de Burgos.
‡ Technical University of Denmark.
§ Universidad de Valladolid.

10.1021/jp800247n CCC: $40.75
Published on Web 06/26/2008

cationic gold clusters, MAu_n^+, depending on the type of atomic impurity (M = Ti, Fe) on one hand, and with size, on the other hand, for several cluster sizes ($n = 3-7$).

The atomic and electronic structures of doped gold clusters, Au_nM^q, change drastically with respect to those of pure gold clusters Au_n^q and Au_{n+1}^q. The different charge state, $q = -1$, 0, and +1 for anions, neutral, and cationic clusters, respectively, plays an important role as well. Thus, despite the tendency of gold clusters to be planar up to unusually high numbers of atoms ($n = 13$ for anions,[21,22] $n = 11$ for neutrals,[23,24] and $n = 7$ for cations[23–25]), it has been shown[26] that the ground-state geometry of MAu_n^+ cations (M = Sc, Ti, V, Cr, Mn, Fe) produced in photofragmentation experiments[27] is not planar for $n > 6$. Similarly, the structure of $Au_{12}W$, $Au_{12}Mo$, and $Au_{12}V^-$ was probed to be icosahedra, with the impurity atom at the center of the cluster.[28] In a previous work, we showed that the electronic and magnetic properties of Au_nM^+ vary in a nonsmooth manner, for each transition metal impurity, when the size of the cluster increases. For example, photofragmentation experiments[24] for MAu_n^+ in the range of $n = 3-9$ show peaks at $n = 5$ (M = Ti, Fe), $n = 7$ (M = Fe), and $n = 2$, 8 (M = Au), which was rationalized from first principles calculations as an effect of closed electronic shells and attributed to maxima in the second difference of the total energy.[23] With respect to the catalytic properties of doped gold clusters, a drastic change as compared to those of pure gold clusters is expected, as shown recently for the case of the anionic $Au_{12}V^-$ cluster.[29] Other recent investigations have demonstrated that the adsorption of atomic oxygen on Pt clusters doped with Ni occurs with a higher binding energy than for pure Pt clusters.[30] In this context, we mention a recent work concerning the effect of Ni and Pd impurity atoms on the geometry, electronic properties, and active sites of copper clusters.[31] On the other hand, it is generally accepted that sites with low coordinated atoms have an enhanced reactivity. We also know, after the experiments of Kim and Ganteför,[32] that nondissociative adsorption of diatomic molecules (N_2 specifically) on nanoclusters can be favored at room temperatures instead of dissociative chemisorption. It is worth mentioning a recent result stating that gold behaves as hydrogen when interacting with halogen atoms,[33] that is, with atoms having a much larger electronegativity than gold.

The roll of oxygen in the oxidation of CO mediated by supported[34] and gas phase[35] gold clusters is still not well-understood, in particular the question as to if that process is ruled by molecular or dissociated forms of oxygen. Some interesting questions are as to what mechanism promotes the adsorption, what the adsorption site of the cluster substrate is, and what the oxidation state of gold is in the reaction. In general, gold clusters that are able to donate electrons interact well with O_2 and, upon adsorption, lead to activation of this molecule by elongation of the O−O bond distance. In other words, it is produced the formal reduction of molecular oxygen to the superoxide state, O_2^-. As a consequence, the adsorption of molecular oxygen on positively charged small gold clusters is not observed experimentally, and the extrapolated binding energy is very small (<0.5 eV).[36] This fact was theoretically confirmed by Ding and co-workers.[15]

The support-specific aspects of oxidation catalysis mediated by gold clusters were studied recently by Laureen and Linic,[37] in particular, the conflicting findings regarding the oxidation state of catalytically active gold atoms (neutral Au^0, cationic $Au^{\delta+}$, or anionic $Au^{\delta-}$). Thus, ultrahigh vacuum (UHV) experiments and DFT calculations[38] showed that adsorbed gold on metal oxides is negatively charged, while steady-state studies[39] suggested that the activity of the Au/oxide catalyst is directly proportional to the concentration of cationic Au atoms. A recent DFT calculation of the charge on small gold clusters supported on partially reduced rutile TiO_2 (110) showed that clusters are not always negatively charged, depending on the size, isomer geometry, and oxygen vacancy type.[40,41] Simply, $Au^{\delta-}$ is needed to adsorb and activate O_2. However, as more and more gold−oxygen bonds are formed, the electronic fingerprint of Au is reversed from anionic to cationic due to the higher oxygen electronegativity. For the sake of completeness, let us mention that recent time-of-flight secondary mass spectroscopy experiments[34,42] provided direct evidence of oxidized gold on supported Au/γ-Al_2O_3 and Au/TiO_2 catalysts, in the form of AuO^-, AuO_2^-, and $AuOH^-$ ion clusters.

With regard to the debate over the presence of metallic gold or cationic gold as the active species, Bond and Thompson proposed that both Au_3^+ and Au^0 are required.[43] In agreement with this type of mechanism, Gates and Guzman found that in active CO oxidation of gold catalysts on MgO supports, both cationic and neutral gold species were present.[44] The same mechanism, involving the presence of both metallic and oxidic gold, is supported by other researchers.[45,46] Bond and Thompson[43] further speculated that the mechanism may not be the same on all supports. Clearly, this is an area that demands more attention and should be an area where contributions from surface science can play a role.[47]

In the second section of this paper are given details of the computational methods used through this work. In the third section are presented and discussed the results for structural and electronic properties of $(Au_nO_2^+)_{ad}$ and $(MAu_nO_2^+)_{ad}$ complexes formed by the adsorption of O_2 on pure (section 3.1.) and doped (section 3.2.) cationic gold clusters, including a comparison of both sets of results. In section 3.3. are discussed results for $(MAu_nO_2^+)_{dis}$ complexes with equilibrium configurations formed with two separated O atoms. Summary and conclusions are given in the fourth section.

Computational Methods

Electronic calculations were performed using the first principles code SIESTA.[48] The electronic structure is described within the spin dependent generalized-gradient approximation (GGA) for the exchange-correlation potential.[49] We used standard norm-conserving pseudo-potentials[50] generated with the valence configuration $2s^22p^4$ for O and the semi-core valence configurations $5d^{10}6s^16p^0$ for Au and $4s^23p^63d^n$ for Ti ($n = 2$) and Fe ($n = 6$). The core radii for s, p, and d orbitals, are in au (2.47, 2.98, 2.00), (2.58, 1.09, 1.38), (2.47, 0.99, 0.99), and (1.14, 1.14, 1.14) for Au, Ti, Fe, and O, respectively. Flexible linear combinations of numerical pseudo-atomic orbitals (PAO) are used as the basis set, allowing for multiple-ξ and polarization orbitals. To limit the range of PAOs, they were slightly excited by a common energy shift (here we took 0.001 Ry) and truncated at the resulting radial node, leading to a maximum cutoff radii, in au, of 8.63 (s), 10.06 (s), 8.95 (s), and 5.72 (p) for Au, Ti, Fe, and O, respectively. These basis sets were used and tested in previous works.[24,26] In the present calculations, we used a double-ξ s,p,d basis plus a single p polarization orbital (DZP) for Au, Ti, and Fe. We checked that by using a triple-ξ s,p,d basis plus polarization (TZP), the absorption energy of O_2 on top of M in the Au_3M^+ cluster increases only 0.02 eV with respect to the DZP calculation for both M = Ti, Fe complexes. This test indicates that the basis set superposition error is also small. A general discussion about the performance of different multiple-ξ basis sets in the context of SIESTA code calculations

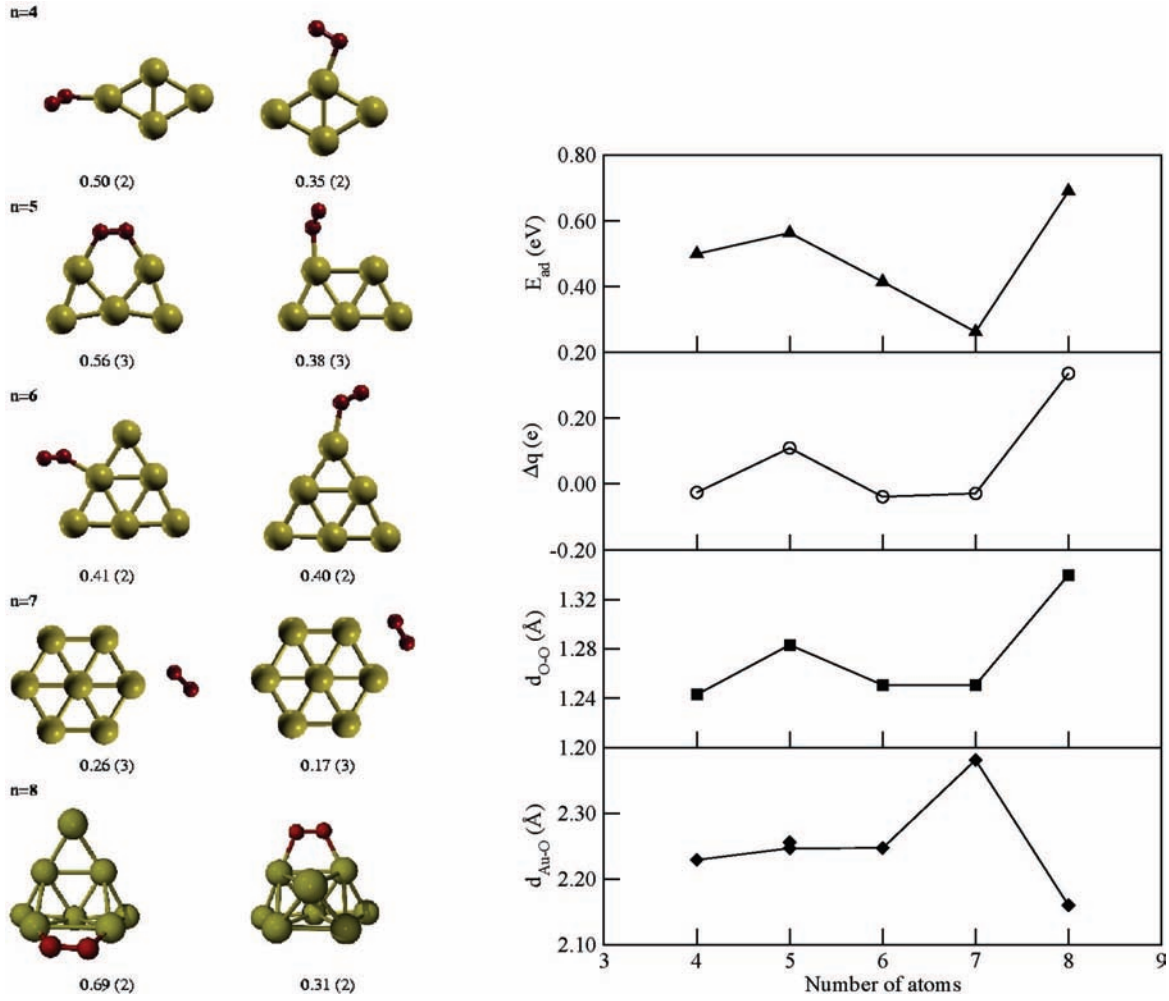

Figure 1. Left: two lowest energy isomers of $Au_nO_2^+$ clusters for $n = 4-8$. Small spheres represent oxygen atoms. Below each structure are given the adsorption energy of O_2, in eV (eq 1), and the total spin multiplicity (in parentheses). Right: from top to bottom, adsorption energy of O_2, E_{ad}, in eV (▲), excess of charge on O_2, Δq, in electron units (○), distance O−O, in Å (■), and distance Au−O_2, in Å (♦). For $Au_5O_2^+$, there are given two Au−O_2 distances because the planar Au_5^+ geometry becomes slightly nonplanar after O_2 adsorption.

in comparison to the number of plane-waves and cutoff energy used in first principles plane-wave-type of calculations to achieve analogous convergence and accuracy against experiments is given in ref 48(see Figure 2 of ref 48).

The basis functions and electron density were projected onto a uniform real space grid to calculate the Hartree and exchange correlation potentials and matrix elements. The grid fineness is controlled by the energy cutoff of the plane-waves that can be represented in it without aliasing (here, we take 120 Ry). The geometry was optimized within a conjugate-gradient method until the force on each atom was smaller than 0.010 eV/Å. We tested several different initial positions for the adsorbed molecule.

Results and Discussion

Adsorption of O_2 on Pure Cationic Au_n^+ Clusters. In Figure 1 are represented the two lowest energy equilibrium configurations of $Au_nO_2^+$ complexes obtained from full relaxation of several initial geometries composed of an O_2 molecule added to the low lying energy isomers of Au_n^+ clusters obtained in a previous work. The gold cluster suffers almost no distortion after oxygen adsorption. In particular, the planarity of Au_n^+ is preserved in the complex $Au_nO_2^+$ up to $n = 7$. Let us mention for future reference that an almost degenerate three dimensional isomer of Au_7^+ also was reported. For $n = 4$, 6, and 7, the O_2 molecule is adsorbed on top of a low coordinated Au atom forming an angle of ∼118−120° with the cluster plane, and the O−O bond line points towards the empty side of the complex. For $n = 5$ and 8 clusters, the largest adsorption energy was obtained for O_2 in the bridge configuration. The adsorption energy of one O_2 molecule on a cationic pure gold cluster is calculated as

$$E_{ad}(n) = E[(Au_n^+)_{GS}] + E[O_2] - E[(Au_nO_2^+)_{ad}] \quad (1)$$

Here, $E[(Au_n^+)_{GS}] + (E[O_2])$ is the total energy of the cluster (O_2 molecule) for the ground-state isomer, and $E[(Au_nO_2^+)_{ad}]$ is the total energy of the $(Au_nO_2^+)_{ad}$ complex in a given energy equilibrium configuration. The two isomers of $(Au_nO_2^+)_{ad}$ with a lower energy for each size n are represented in Figure 1, where $E_{ad}(n)$ is given below each structure. For the top adsorption of O_2 on the edge or vertex Au atoms of a triangular Au_6^+ ground-state geometry, nearly the same value of $E_{ad}(6)$ is obtained. The configuration $Au_4O_2^+$ in Figure 1 is similar to that obtained by Ding et al.,[15] but different from that obtained by Joshi et al.,[17] which bound O_2 to Au in the smaller diagonal of rhombic Au_4^+. On the other hand, Ding et al.,[15] found for $Au_5O_2^+$ a top adsorption configuration instead of the bridge configuration obtained in this work.

The adsorption energy $E_{ad}(n)$ is represented versus the cluster size in the top panel at the right of Figure 1. In the second panel

is given the excess of charge on adsorbed O_2, Δq, in units of the charge of an electron. We see that Δq is positive (negative) in the case of adsorption on bridge (top) sites. A positive (negative) Δq means that the electronic charge flows towards (from) O_2. In the third panel at the right of Figure 1 is represented the distance O−O after adsorption of O_2, which follows a trend similar to that for Δq shown previously, that is, the O−O distance and charge on O_2 are larger for bridge configurations than for the top configurations. Thus, adsorption of O_2 on the bridge positions leads to the superoxo molecular state, ready, for example, for CO oxidation. Notice that the adsorption energy in these bridge positions is larger than 0.5 eV, which is the estimated limit for experimental observation according to signal-to-noise limitations.[13,36] The trend with the cluster size of O−O distances correlates also with $E_{ad}(n)$: the larger the O−O distance is, the larger the adsorption energy is. The results for the Au−O_2 distance after oxygen adsorption are represented in the lower panel at the right of Figure 1. The distance of Au−O_2 (adsorption energy) for $Au_7O_2^+$ is larger (smaller) than for $Au_8O_2^+$. The low reactivity of cationic Au_7^+ towards O_2 is due to the high stability conferred to a planar structure by six valence electrons, which is a magic number (due to closed electronic shells) for a planar spherically symmetric configuration. The small adsorption energy of the bridge configuration of $Au_7O_2^+$ in Figure 1, 0.17 eV, is only slightly larger than for the on top $Au_7O_2^+$ complex obtained from the three dimensional isomer of Au_7^+ mentioned previously, not represented in Figure 1.

The calculated spin multiplicity of the $Au_nO_2^+$ structures in Figure 1 is given in parentheses below the corresponding isomer. Those Au_n^+ cations with an even number of atoms have an odd number of electrons, and the corresponding ground state is a doublet. The spin 1/2 of these clusters couples anti-parallel to spin 1 of the adsorbing O_2 molecule, resulting in a spin doublet for $Au_nO_2^+$ structures with $n = 4$, 6, and 8. For $n = 5$ and 7, the Au_n^+ cations have spin zero, and after adsorbing O_2, it results in a triplet spin state for the lowest energy $Au_nO_2^+$ complex.

Comparing the results for O_2 adsorption on Au_n^+ clusters shown in Figure 1 with those for neutral and anionic gold clusters obtained in previous papers[9,12] in the same range of sizes, we see that (i) O_2 adsorption energies are similar to those for neutral clusters but smaller than for anionic gold clusters; (ii) contrary to neutral and anionic species, there are not odd−even effects in the adsorption energy of $Au_nO_2^+$; (iii) the adsorption energy of Au_n^- anions is always higher for top positions than for bridge positions, but the opposite occurs for neutral Au_n with $n = 5$ and 7 and for cationic Au_n^+ with $n = 5$ and 8; and (iv) for neutral Au_nO_2 complexes, electrons flow from Au to O_2 independently of the configuration of the ground state, whereas for $Au_nO_2^+$, electrons flow from Au to O_2 for bridge configurations and in the opposite direction for top configurations.

The equilibrium configurations $(Au_nO_2^+)_{dis}$ resulting from optimization of complexes formed by adding two O atoms at different sites of the Au_n^+ ground-state geometry also were calculated. In many cases, the two O atoms formed initially an O_2 molecule that forced Au−O distances that were much smaller than those shown in the lowest panel of Figure 1 and from that evolved to an equilibrium configuration with two separated O atoms. But, in other cases, the initial configuration already was formed with two separated O atoms at several sites. To compare the stability of these $(Au_nO_2^+)_{dis}$ and $(Au_nO_2^+)_{ad}$ complexes with respect to the fragmentation in Au_n^+ and O_2, we calculated the quantity $E_{dis}(n)$, defined, similarly to $E_{ad}(n)$ of eq 1, as

$$E_{dis}(n) = E[(Au_n^+)_{GS}] + E[O_2] - E[(Au_nO_2^+)_{dis}] \quad (2)$$

Here, $E[(Au_nO_2^+)_{dis}]$ is the lowest equilibrium energy of $(Au_nO_2^+)_{dis}$ complexes for a given n, $E[O_2]$ is the ground-state energy of O_2, and $E[(Au_n^+)_{GS}]$ is the ground-state energy of Au_n^+. From the present calculations, it was found that $E_{dis}(n)$ is smaller than $E_{ads}(n)$ for all sizes n. Actually, $E_{dis}(n)$ is always negative except for $(Au_6O_2^+)_{dis}$, which yields a small positive value $E_{dis}(6) = 0.34$ eV.

Molecular Adsorption of O_2 on Doped MAu_n^+ Clusters. In Figures 2–5 are represented several equilibrium geometries of those complexes $(MAu_nO_2^+)_{ad}$ formed by adsorbing O_2 on different sites of a few low lying energy isomers of doped gold clusters MAu_n^+. These initial isomers, which were obtained in a previous work, are represented in the first column of Figures 2–5. Except for $n = 6$, the ground-state geometry of MAu_n^+ clusters is the same for Ti and Fe impurities. All initial MAu_n^+ isomers are planar except for isomer III of MAu_6^+ as well as those of MAu_7^+. For both Ti and Fe doped clusters, the difference of binding energy per atom of the initial MAu_n^+ isomers with respect to that of the ground state, as well as the spin multiplicity (in parentheses), is given below each geometry. The different equilibrium geometries of $(MAu_nO_2^+)_{ad}$ complexes for the various types of adsorption configurations are depicted in separate columns of Figures 2–5, with the adsorption energy and spin multiplicity (in parentheses) given below each structure. The O_2 adsorption energy is defined, similarly to eq 1, as

$$E_{ad}(n) = E[(MAu_n^+)_{GS}] + E[O_2] - E[(MAu_nO_2^+)_{ad}] \quad (3)$$

Here, $E[(MAu_n^+)_{GS}]$ is the total energy of the ground-state isomer, which does not necessarily coincide with the energy of the initial isomer leading to the given equilibrium configuration, and $E[(MAu_nO_2^+)_{ad}]$ is the total energy of the given complex. For example, the adsorption energy for the on top complex $TiAu_nO_2^+$ in the second row of Figure 3, 2.52 eV, should increase to 2.64 eV when referred to the total energy of isomer II of MAu_5^+. The different adsorption configurations are identified in columns 2−5 as on top M 1, bridge M-Au, on top Au, and bridge Au-Au, respectively. We distinguish two cases for the on top M configuration: on top M 1, which has the two oxygen atoms bonded to the M impurity, and on top M 2, which has only one O atom of O_2 bonded to M.

A few general features about the structure of $(MAu_nO_2^+)_{ad}$ complexes are extracted from Figures 2–5 and summarized in this paragraph. The highest adsorption energy corresponds always to the on top M 1 complexes. These on top M 1 complexes are formed without a severe distortion of the MAu_n^+ initial cluster geometry. For M = Ti, the second preferred configuration is that of bridge M-Au type, but when M = Fe, this configuration has a similar or smaller adsorption energy than the bridge Au-Au and/or on top Au complexes. For the more favorable on top M and bridge M-Au configurations, it was found that $TiAu_n^+$ is more active toward O_2 than $FeAu_n^+$ clusters. Those on top M 1 type complexes arising from the ground-state isomer $(MAu_n^+)_{GS}$ have the highest adsorption energy, except for $(MAu_6O_2^+)_{ad}$ and $(FeAu_7O_2^+)_{ad}$, which are formed from low lying energy isomers. As will be detailed in the following paragraphs, the highest adsorption energy configuration for a given size n combines with a lower atomic coordination of M, a smaller value of the O−M distance, and a larger gain of electron charge on O_2 than for other configurations. The behavior of the spin multiplicity of $(MAu_nO_2^+)_{ad}$ complexes with dependence on M and n will be commented on next and later in connection with Figure 6.

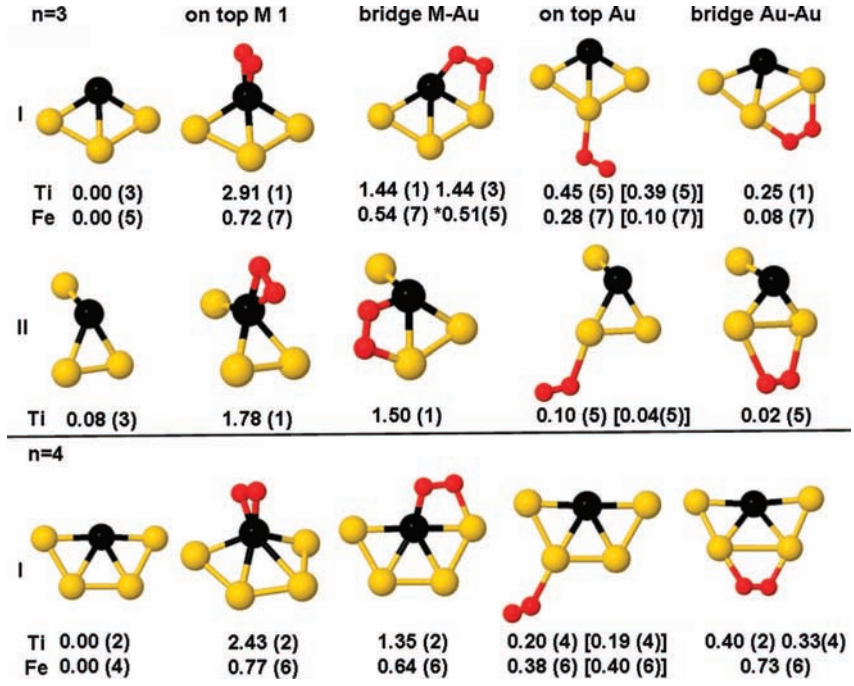

Figure 2. Equilibrium geometries of $(MAu_nO_2^+)_{ad}$ complexes formed by molecular oxygen adsorbed on MAu_n^+ clusters for M = Ti, Fe and n = 3−4. The black sphere represents the M impurity, and the two small spheres represent the O_2 molecule. The first column shows the initial MAu_n^+ isomers from ref 26, whose excess of binding energy per atom with respect to the ground state (in eV) is given below each structure for Ti and Fe doped clusters. The spin multiplicity also is given (in parentheses). The other columns correspond to different equilibrium adsorption configurations as indicated. The adsorption energy, in eV (eq3), and the spin multiplicity (in parentheses) are given below each $(MAu_nO_2^+)_{ad}$ complex. The data in square brackets for the on top Au site correspond to O_2 adsorbed on the other nonequivalent Au atom. The data with asterisks for the bridge M-Au site correspond to a geometry slightly distorted from the represented one. For the bridge Au-Au $(TiAu_4O_2^+)_{ad}$ complex are given two isomers with the same geometry and different E_{ad} (multiplicity) values.

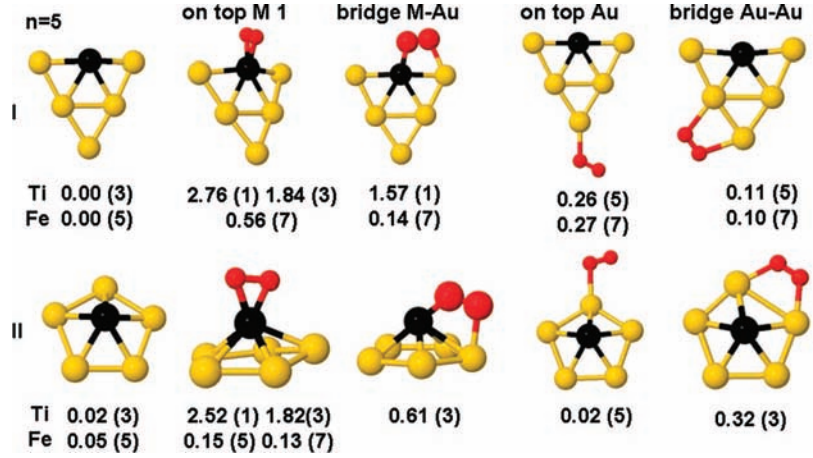

Figure 3. Same as Figure 2 for structures of $(MAu_5O_2^+)_{ads}$ complexes formed from the two lower energy isomers of Au_5M^+ clusters I and II in the first column, respectively. For on top M 1 configurations are given two sets of data corresponding to nearly the same geometry and different adsorption energies and multiplicities.

In Figure 2 are represented the fully optimized geometries of complexes $(MAu_nO_2^+)_{ad}$ for n = 3 and n = 4. Two initial isomers of MAu_n^+ were considered for n = 3, and only one for n = 4, which are depicted in the first column. As already was noted, the highest adsorption energy was obtained for the on top M 1 configuration, which has the triangle O−M−O placed vertically to the plane of the MAu_3^+ rhombus and the O−O line nearly parallel to the shorter diagonal of that rhombus. We obtained also an on top M 2 O−O−M configuration (not shown) from isomer I with adsorption energy (spin multiplicity) values of 1.43 eV (1) for M = Ti and 0.45 eV (7) for M = Fe, which are slightly smaller than those for the bridge M-Au complexes from isomer I. The fact that the highest adsorption energy is larger for Ti than for Fe complexes is related to the smaller O−M bond distance of Ti with respect to Fe complexes, as shown in Figure 6, and is due to the larger transfer of electronic charge to O_2 from Ti than from Fe, as expected from relative electronegativity differences among M and O_2. Specifically, by means of Mulliken population analysis, the extra charge on O_2 in $(MAu_3O_2^+)_{ad}$ complexes with the highest adsorption energy is 0.398 electrons for M = Ti and 0.183 electrons for M = Fe. On the other hand, the polarization (spin-up minus spin-down electronic charges) for each of the Au_3, M, and O_2 subsystems of $(TiAu_3O_2^+)_{ad}$ was zero, but it was 0.601, 3.834, and 1.563 electrons, respectively, for $(FeAu_3O_2^+)_{ad}$. The sum of these values leads to a total polarization 2*S*, which is null for

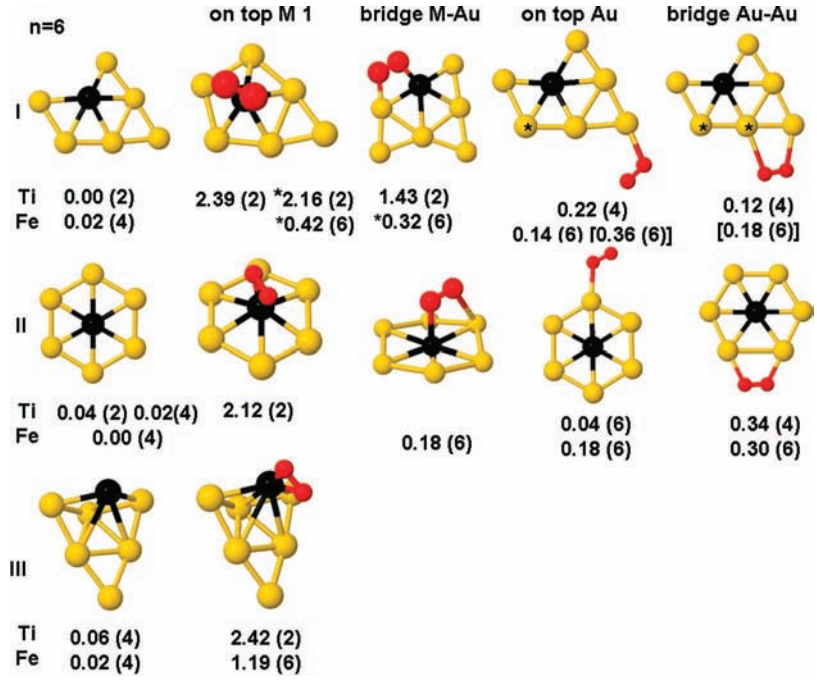

Figure 4. Same as Figure 2 for $(MAu_6O_2^+)_{ads}$ complexes. The complexes with maximum adsorption energy are the on top M 1 type formed from the three dimensional isomer III of MAu_6^+ instead of the planar isomers I and II, which are the ground state of $TiAu_6^+$ and $FeAu_6^+$, respectively. Those data that are marked with an asterisk correspond to equilibrium configurations (not shown) without distortion of the isomer I geometry. The on top M 1 configuration from isomer I is not an equilibrium structure for M = Fe complexes and evolves to the on top M 1 configuration from isomer III.

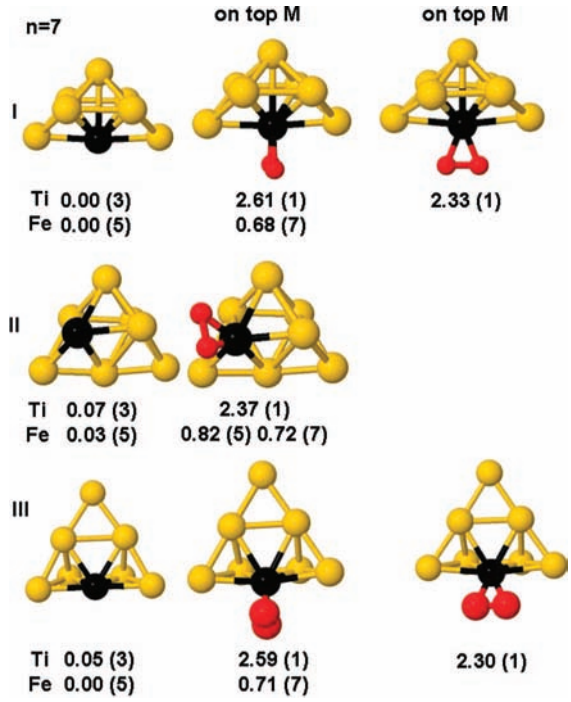

Figure 5. Equilibrium minimum energy configurations of on top M 1 $(MAu_7O_2^+)_{ad}$ complexes obtained from three isomers of MAu_7^+ depicted in the first column. Contrary to previous results for $n < 7$, the complexes $(MAu_7O_2^+)_{ad}$ with a maximum adsorption energy have different structures for M = Fe (which came from isomer II) than for M = Ti (which came from isomer I). Note that the $(FeAu_7O_2^+)_{ad}$ complex with maximum adsorption energy does not have a maximum spin multiplicity as for $n < 7$ complexes, which is due to a combined effect of O−Fe distance and local spin charge on O_2 and Au (see text).

$(TiAu_3O_2^+)_{ad}$ and 6 for $(FeAu_3O_2^+)_{ad}$, and the spin multiplicity $2S + 1$ is 1 and 7, respectively. The Mulliken charges are known to be basis set dependent.[51] To test the importance of that effect in our results, we calculated again $(MAu_3O_2^+)_{ad}$ using a TZP basis resulting in a reduction of 0.06 electrons in the extra charge on O_2 of both M = Ti, Fe complexes with the highest adsorption energy. Similarly, the polarization of the Au_3, M, and O_2 subsystems obtained with TZP calculations was again zero for the M = Ti complex, and it was 0.619, 3.815, and 1.567, respectively, for the M = Fe complex. These values are similar to those from DZP polarization calculations reported previously, giving us confidence in the comparison of Mulliken charges of $(MAu_nO_2^+)_{ad}$ for Ti versus Fe complexes discussed in this work.

In the case of $(MAu_3O_2^+)_{ad}$, we calculated within a triple-ξ plus polarization basis an extra charge on O_2 of 0.330 electrons for M = Ti and 0.135 electrons for M = Fe for complexes with the highest adsorption energy. These values are similar to those from the double-ξ plus polarization calculation reported previously, giving us confidence in the Mulliken charges discussed in this work.

For the $n = 3$ bridge M-Au configuration from isomer I, a second set of data is given in Figure 2. Both sets of data have nearly the same geometry and adsorption energy but different spin multiplicities. Those data for M = Fe marked with an asterisk correspond to a slightly different planar geometry having a shorter small diagonal of the rhombus. Those of complexes having the highest multiplicity for a given M have also the largest O−M distance and the largest O−Au average distance. For example, the O−M distance in bridge M-Au configurations from isomer I is 1.95 (2.16) Å for multiplicity 1 (3) of M = Ti complexes and 2.03 (1.96) Å for multiplicity 7 (5) in the M = Fe case. A similar correlation between the spin multiplicity and the calculated electric dipole moment of these complexes exists. Thus, for the bridge M-Au $TiAu_3O_2^+$ complex from isomer I, the electric dipole moment is 5.14 (5.29) D for multiplicity 1 (3), and for the $FeAu_3O_2^+$ case, the dipole moment is 4.73 (4.24) D for multiplicity 7 (5).

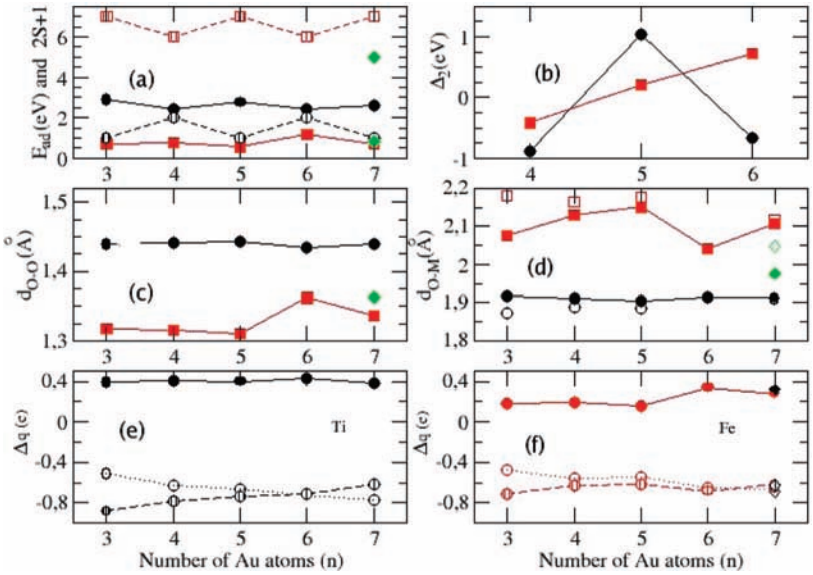

Figure 6. Evolution with cluster size of several properties of those $(MAu_nO_2^+)_{ad}$ complexes with the highest adsorption energy for M = Ti (●) and M = Fe (■). (a) Upper panel left: adsorption energy, in eV, and spin multiplicity, $2S + 1$, (○ for Ti and □ for Fe); (b) upper panel right: second difference of total cluster energy; (c) middle panel left: distance between oxygen atoms after O_2 molecular adsorption; (d) middle panel right: distance from each oxygen atom of adsorbed O_2 to the M impurity; (e) lower panel left: Mulliken charges, in electrons, on Au_n (dashed circles), O_2 (●), and Ti (○) subsystems of $(TiAu_nO_2^+)_{ad}$ complexes; (f) lower panel right: same as panel e for M = Fe. Diamonds in panels a, c, d, and f represent data for the $(FeAu_7O_2^+)_{ad}$ complex with spin multiplicity of 5.

The second set of data, in square brackets, for the on top Au $MAu_3O_2^+$ complex from isomer I, correspond to configurations with O_2 adsorbed on the other nonequivalent Au atom of MAu_3^+. These configurations have the same spin multiplicity as the first one but a smaller adsorption energy and larger O−Au distance. Thus, for M = Ti, that distance is 2.40 (2.52) Å for the complex with an adsorption energy of 0.45 (0.39) eV, and for M = Fe, the O−Au distance is 2.36 (2.63) Å for the complex with an adsorption energy of 0.28 (0.10) eV. For the AuO_2^+ molecule, a triplet state was obtained recently[52] by means of B3LYP (MP2) calculations, with an adsorption energy of 0.49 (0.30) eV, distance O−O of 1.20 (1.20) Å, distance Au−O of 2.34 (2.39) Å, and angle Au−O−O of 125.2° (133.7°). These values are similar to those obtained here for on top Au configurations of $MAu_3O_2^+$ and $Au_4O_2^+$ complexes. Thus, the main role of additional atoms in these complexes is to change the multiplicity 3 of (AuO_2^+) to 2 for $(Au_4O_2^+)$, to 5 for $(TiAu_3O_2^+)$, and to 7 for $(FeAu_3O_2^+)$.

Comparison of the two results for on top Au $MAu_3O_2^+$ from isomer I with the two results that are analogous for on top Au configurations of $Au_4O_2^+$ given in Figure 1 indicates that the adsorption energy is similar (smaller) for $TiAu_3O_2^+$ $(FeAu_3O_2^+)$ than for $Au_4O_2^+$. Thus, the main difference between these $MAu_3O_2^+$ and $Au_4O_2^+$ complexes is that the substitution of an Au atom of $Au_4O_2^+$ by the M impurity turns the spin coupling mode with the O_2 molecule from anti-parallel to parallel. On the other hand, the bridge Au-Au configurations of $(MAu_3O_2^+)_{ad}$ and $Au_4O_2^+$ (not represented in Figure 1) have very small adsorption energies. When the bridge Au-Au $(TiAu_3O_2^+)_{ad}$ complex from isomer I is forced to a spin multiplicity of 5, it evolves to the on top Au equilibrium configurations already discussed. With respect to the complexes $(TiAu_3O_2^+)_{ad}$ from isomer II, the same tendencies as for complexes from isomer I are found. The equilibrium configurations for $(FeAu_3O_2^+)_{ad}$ from isomer II have a negative adsorption energy ($E_{ad} < 0$), that is, they are unstable against fragmentation in a free O_2 molecule and the ground-state isomer I of $FeAu_3^+$.

Analysis of results for $(MAu_4O_2^+)_{ad}$ complexes, which are given also in Figure 2, leads to analogous considerations as for $(MAu_3O_2^+)_{ad}$ complexes. We see that the adsorption energy for on top Au and bridge Au-Au configurations of $(MAu_4O_2^+)_{ad}$ is smaller than that for similar $Au_5O_2^+$ complexes of Figure 1. An exception is the near planar bridge Au-Au $(FeAu_4O_2^+)_{ad}$ complex, which has an adsorption energy only slightly smaller than that of the on top M 1 $(FeAu_4O_2^+)_{ad}$ complex. The dipole moment of that bridge Au-Au configuration is 7.28 D as compared to 4.03 D for the on top M 1 complex. Although both of these $(FeAu_4O_2^+)_{ad}$ complexes have spin multiplicities of 6, the distribution of charge is quite different as revealed from Mulliken population analysis. Thus, in the bridge Au-Au configuration, O_2 takes more (less) electrons from Au (Fe) than in the on top M 1 configuration, with a total result of 0.253 electrons for the bridge Au-Au case versus 0.191 electrons for the on top M 1 case. Aside from this, the total spin polarization (difference of spin-up and spin-down electronic charge) of Au atoms is negative ($-0.278\ e^-$) for the on top M 1 complex, but it is positive ($0.144\ e^-$) for the planar bridge Au-Au configuration of $(MAu_4O_2^+)_{ad}$.

At this point, it is worth comparing the dependence with M observed for the spin multiplicity of $(MAu_nO_2^+)_{ad}$ complexes. Firstly, we consider the complexes in the first row in Figure 2. For M = Ti within the on top M and bridge M-Au configurations, the multiplicity is 1 (singlet), which corresponds to an anti-ferromagnetic (anti-parallel)-like coupling of spin 1 of $TiAu_3^+$ with spin 1 of O_2. On the other hand, the complexes $(FeAu_3O_2^+)_{ad}$ in the first row in Figure 2 have a spin multiplicity of 7 for all configurations, which corresponds to a ferromagnetic coupling of spin 1 of O_2 with spin 2 of the $FeAu_3^+$ cluster. Similar trends are observed for the $n = 4$ complexes, that is, minimum spin (2) for Ti complexes and maximum spin (6) for those of Fe, as well as for those with $n = 5-7$ in Figures 3–5, which will be commented on and discussed next. The $(FeAu_nO_2^+)_{ad}$ complex with the highest adsorption energy configuration has a multiplicity of 7 (6) for odd (even) n, and the total energy difference with the complex having the same configuration but lower multiplicity (given in parentheses) is (in eV) 0.98 (3) and 1.20 (1) for $n = 3$, 0.32 (2) for $n = 4$, 0.28 (3) and 1.34 (1) for $n = 5$, 0.47 (2) for $n = 6$, and 0.66 (3) and

0.42 (1) for $n = 7$. For low adsorption energy sites, namely, on top Au and bridge Au-Au of $(TiAu_nO_2^+)_{ad}$ in Figure 2, the spin multiplicity is the largest possible, corresponding to a ferromagnetic-like coupling of the spins of O_2 and $TiAu_n^+$ clusters, with exceptions of the bridge Au-Au $(TiAu_nO_2^+)_{ad}$ complexes with $n = 3$ and 4 (isomer I) and $n = 5$ (isomer II).

In Figure 3 are given the adsorption energy and spin multiplicity for $(MAu_5O_2^+)_{ad}$ complexes within different equilibrium configurations, displayed as in Figure 2. Although isomers I and II of MAu_5^+ are nearly degenerate, the complexes arising from isomer I are more stable than those arising from isomer II, except for the bridge Au-Au configuration of $(TiAu_5O_2^+)_{ad}$. For each type of configuration, O_2 is adsorbed preferably on low coordination sites of M or Au. The bridge Au-Au $(TiAu_5O_2^+)_{ad}$ complex from isomer II, which has a spin multiplicity of 3, evolves to the on top Au type when it is forced to multiplicity 5. On the other hand, the bridge M-Au configuration from isomer II for M = Fe (not shown) has a negative adsorption energy, $E_{ad} = -0.26$ eV, that is, the $(FeAu_5O_2^+)_{ad}$ complex is not stable against fragmentation in $FeAu_5^+$ and O_2 fragments. The bridge M-Au $(TiAu_5O_2^+)_{ad}$ complex is a triplet and evolves towards the on top M configuration II when it is forced to be a singlet. For the on top Au and bridge Au-Au sites, there are several nonequivalent Au positions, but in Figure 3 only those cases with the largest adsorption energy are provided. For example, for the on top Au case with O_2 placed at the corner closest to the impurity M = Ti, the calculated adsorption energy is 0.16 eV, with a spin multiplicity of 5.

The highest adsorption energy of $(MAu_5O_2^+)_{ad}$ complexes occurs for the on top M 1 site and is larger for Ti than for Fe doped clusters. We found several isomeric on top M 1 $(TiAu_5O_2^+)_{ads}$ complexes with identical geometries but different adsorption energies and spin multiplicities. This results in that the increase of the multiplicity of on top M 1 complexes without appreciable change of geometry leads to a decrease in the adsorption energy. Thus, from isomer I of $TiAu_5^+$, three on top M 1 complexes are found, having O_2 adsorption energies (spin multiplicities) of 2.76 (1), 1.84 (3), and 0.30 (5), respectively. Similarly, for M = Ti complexes from II are found three equilibrium on top M 1 complexes with adsorption energies (multiplicities) of 2.52 (1), 1.82 (3), and 0.66 (5), respectively. However, the opposite occurs for $(FeAu_nO_2^+)_{ads}$ complexes, as already was commented. Particularly, those on top M 1 $(FeAu_5O_2^+)_{ad}$ complexes from isomer I are forced to a lower spin multiplicity than 7 evolve to bridge M-Au equilibrium configurations. From a detailed Mulliken population analysis of those spin-isomers of on top M $(MAu_nO_2^+)_{ads}$ complexes for a given size, the highest adsorption energy configuration correlates with the highest electron charge on the O_2 molecule.

In Figure 4 are given the results for $(MAu_6O_2^+)_{ad}$ complexes as in Figures 2 and 3. Isomer I is the ground state of $TiAu_6^+$, and isomer II is the ground state of $FeAu_6^+$. Isomer II of $TiAu_6^+$ has two nearly degenerate states with similar geometries and binding energies but different spin multiplicities, the largest multiplicity being related to the largest Ti−Au average distance. Specifically, the isomer with a multiplicity of 4 (2) corresponds to a Ti−Au average distance of 2.78 (2.76) Å. On the other hand, isomer III of MAu_n^+ is the first nonplanar isomer considered in this work, and its structure is similar to that of the three dimensional isomer of Au_7^+ (not depicted in Figure 1) mentioned at the beginning of this section. Interestingly, those $(MAu_6O_2^+)_{ad}$ complexes with the largest adsorption energy arise from the nonplanar isomer of MAu_6^+. Those data for on top M 1 complexes from isomer I that are marked with an asterisk correspond to equilibrium configurations (not shown) without appreciable distortion of the isomer I structure. The on top M 1 configuration from isomer I depicted in Figure 4 is not an equilibrium structure for M = Fe and evolves to the on top M 1 structure from isomer III. Two equilibrium on top M 2 configurations of $FeAu_6O_2^+$ (not shown) were found, with an adsorption energy (multiplicity) of 0.28 eV (6) from isomer I and 0.18 eV (6) from isomer II, respectively. The on top M 1 configuration from isomer II was not found for M = Fe, and the bridge M-Au from isomer II for M = Ti evolved to the on top M 1 type.

For the on top Au and bridge Au-Au $(FeAu_6O_2^+)_{ad}$ configurations from isomer I, the values given in square brackets correspond to adsorption positions on those Au atoms marked with an asterisk. For bridge Au-Au complexes, the second position is the only one found for M = Fe, whereas it was not found for M = Ti. The behavior of the spin multiplicity with respect to the adsorption configuration is similar to that in Figures 2 and 3 for complexes with $n = 3-5$. Similarly, the relations between adsorption energy with O−M distances and dipole moments for the different complex configurations fulfill the same trends. On the other hand, comparison of $(MAu_6O_2^+)_{ad}$ complexes from isomer II with those $(Au_7O_2^+)_{ad}$ complexes of Figure 1 having a similar structure shows that the impurity in the doped cluster enhances (decreases) the O_2 adsorption energy for the bridge Au-Au (on top Au) configuration with respect to that of the pure cluster.

In Figure 5 are presented five on top M 1 adsorption geometries of $(MAu_7O_2^+)_{ad}$ complexes arising from three nonplanar isomers of MAu^+ clusters. From each one of isomers I (ground state) and III was obtained two on top M 1 configurations when M = Ti, which differs in the orientation of O_2 relative to the initial cluster. Instead, for M = Fe complexes from isomers I and III (which are nearly degenerate), only one of these on top M 1 complexes has a positive adsorption energy. Those $(FeAu_nO_2^+)_{ad}$ complexes for $n < 7$ with the highest adsorption energy have the highest possible value of multiplicity. However, in the case of the on top M 1 $(FeAu_7O_2^+)_{ad}$ configuration from isomer II, two nearly degenerate complexes were obtained, with multiplicities of 5 and 7, respectively, and that with the highest spin had the smallest adsorption energy. (A similar situation occurred for the two $(FeAu_5O_2^+)_{ad}$ complexes from isomer II reported in Figure 4, although these cases are not the highest adsorption energy complexes.) Specifically, for the $(FeAu_7O_2^+)_{ad}$ complex with an adsorption energy of 0.82 (0.72) eV, the spin multiplicity is 5 (7), O−Fe is 1.99 (2.11) Å, excess charge on O_2 is 0.318 (0.281) electrons, and the spin-up minus spin-down electronic charge difference on O_2, Au_7, and Fe subsystems of the complex are 1.07 (1.45), −0.55 (0.74), and 3.48 (3.81) electrons, respectively. Comparison of these values for the two on top M 1 $(FeAu_7O_2^+)_{ad}$ complexes from isomer II agrees with the tendencies studied previously.

The following magnitudes of those $(MAu_nO_2^+)_{ad}$ complexes with a maximum O_2 adsorption energy are represented in Figure 6 for $n = 3-7$: (a) O_2 adsorption energy and spin multiplicity (upper left panel); (b) second difference of total energy with respect to n (upper right panel); (c) distance O−O after adsorption of an O_2 molecule (middle left panel); (d) distances O−M of each O atom of O_2 to atom M (middle right panel); (e) and (f) electronic charge on Au_n, M, and O_2 subsystems, according to Mulliken population analysis, for M = Ti (lower left panel) and M = Fe (lower right panel).

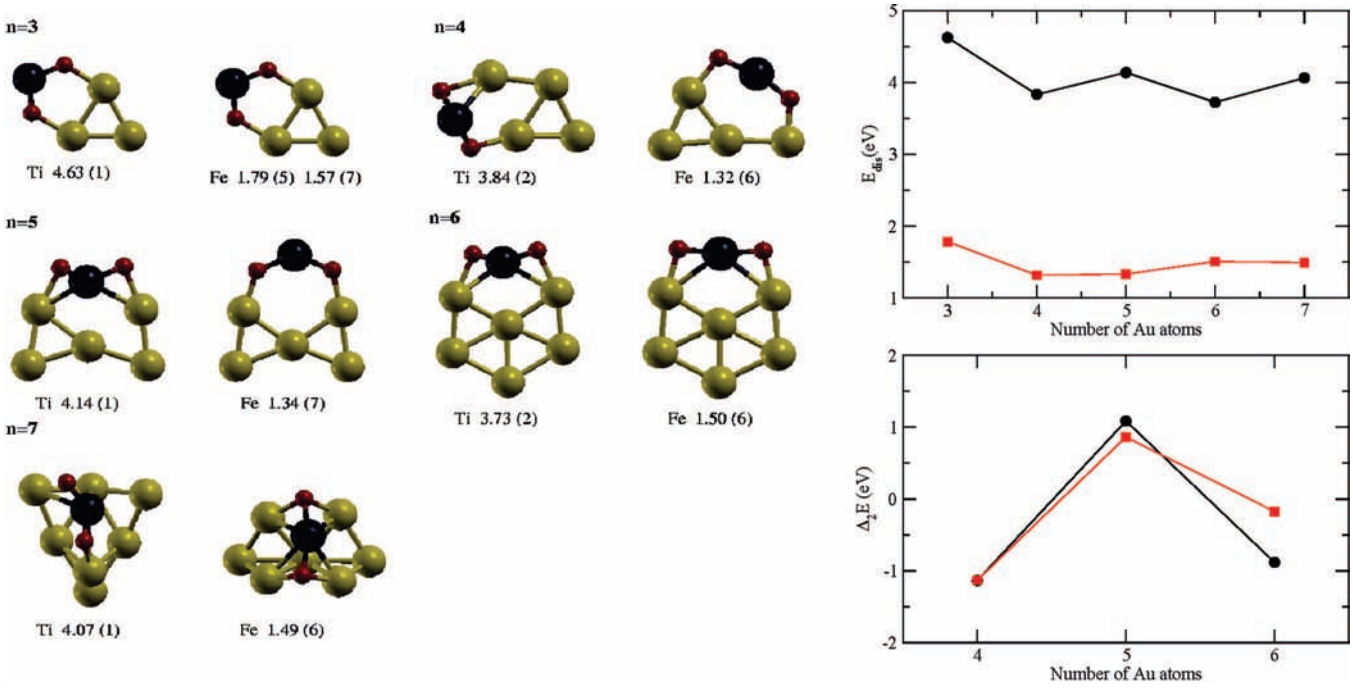

Figure 7. In the left part are represented the minimum energy equilibrium configurations of $(MAu_nO_2^+)_{dis}$ complexes ($n = 3-7$ and M = Ti, Fe), which are formed by optimizing initial configurations of MAu_n^+ in the ground state with two separated oxygen atoms added at different cluster atoms. The black sphere represents the impurity atom, and the two small spheres represent the oxygen atoms. The geometry of the initial lowest energy isomer of the Au_n^+M cluster, which is shown in Figures 2–5, became deformed after adsorption of the two separated oxygen atoms. The adsorption energy, in eV, calculated with respect to the lowest energy isomer of MAu_n^+ and a free O_2 molecule (eq 5), and the spin multiplicity $2S + 1$ (in parentheses), are given below each structure. In the upper right panel is represented the adsorption energy for Ti (●) and Fe (■) doped clusters as a function of cluster size. The second difference of the total cluster energy (eq 4) is represented in the lower right panel, showing a peak at $n = 5$ for both M = Ti and M = Fe doped $(MAu_nO_2^+)_{dis}$ complexes.

The highest adsorption energy is larger for M = Ti than for M = Fe, which is due mainly to electronic effects because the equilibrium adsorption configuration is similar for both types of complexes. Thus, the electronegativity difference of M with O is larger for M = Ti than for M = Fe, and the charge transfer between O_2 and $TiAu_n^+$ is larger than between O_2 and $FeAu_n^+$ clusters, as can be seen in panels e and f of Figure 6. The same effect is manifested in the O−M bond distances represented in panel d of Figure 6, which are shorter for Ti than for Fe complexes, leading to a stronger bond. The second difference of the total energy of the complexes, calculated as

$$\Delta E_2(n) = E[(MAu_{n+1}O_2^+)_{ad}] + E[(MAu_{n-1}O_2^+)_{ad}] - 2E[(MAu_nO_2^+)ad] \quad (4)$$

is represented in the upper right panel of Figure 6. We see that $\Delta E_2(n)$ shows a peak at $n = 5$ for M = Ti, which means that $(TiAu_5O_2^+)_{ad}$ is a very stable complex in comparison to its neighbours at $n = 4$ and 6.

On the other hand, the odd−even effect of the adsorption energy is opposite for Ti than for Fe complexes, despite that in both Ti and Fe series the number of valence electrons is odd (even) for n even (odd). That different odd−even effect correlates with the different magnetic configurations of Ti and Fe complexes. To see that, the trend of the spin multiplicity $2S + 1$ of $(MAu_nO_2^+)_{ad}$ complexes is represented by the dotted lines in panel a of Figure 6. As n increases, an odd−even alternation of the spin multiplicity is observed, which is opposite to the odd−even alternation of the adsorption energy, that is, the larger the adsorption energy is, the smaller the spin multiplicity is. For $TiAu_n^+$ before O_2 adsorption, the spin multiplicity is 3 (2) for the odd (even) n cases, which corresponds to an odd (even) number of electrons. After O_2 adsorption, the spin multiplicity decreases to 1 (2) for odd (even) complexes. This feature corresponds to anti-parallel (anti-ferromagnetic) coupling of the spins of the cluster and O_2 molecule. On the other hand, for $FeAu_n^+$ clusters, the spin multiplicity is 5 (4) for n odd (even) and increases to 7 (6) for n odd (even) complexes after O_2 adsorption. This fact corresponds to parallel (ferromagnetic) coupling of the cluster and O_2 spins. Thus, for both Ti and Fe complexes along n = 3−7, the largest energy corresponds to the smallest spin, that is, to the smallest difference among the spin-up and spin-down electron densities compatible with anti-ferromagnetic (ferromagnetic) coupling for Ti (Fe) complexes. Note also that the larger the O−M distance is, the larger the spin multiplicity is. For $(FeAu_7O_2^+)_{ad}$ are depicted in Figure 6 data corresponding to the two near degenerate on top M complexes arising from isomer II, with spin multiplicities of 5 and 7, respectively.

By means of Mulliken population analysis, the spin polarizations (spin-up minus spin-down electronic charge) of the Au_n, M, and O_2 subsystems of $(MAu_nO_2^+)_{ad}$ were obtained for the highest adsorption energy on top M 1 configurations. In the case of M = Ti, these spin polarizations are zero for $n = 3$, 5, and 7 but 0.754, 0.321, and −0.077 electrons, respectively, for $n = 4$ and 0.498, 0.688, and −0.184 electrons, respectively, for $n = 6$. In the case of M = Fe complexes, the polarizations of Au_n, M, and O_2 subsystems are not null and present an odd−even alternation, which is opposite to the odd−even alternation of the total electron charge on each subsystem.

As shown in the left middle panel of Figure 6, the distance among O atoms in the adsorbed molecule is larger for Ti doped complexes than for those doped with Fe and in both cases is larger than for the free O_2 molecule. For M = Ti, that distance

is much larger than for M = Fe, conferring to the O_2 adsorbed molecule the character of a peroxide state. This is confirmed by Mulliken charge analysis in panels e and f of Figure 6, giving an excess charge to the O_2 adsorbed molecule of ~0.4 electrons for M = Ti. For M = Fe complexes, the O−O distance is enhanced when $n = 6$ and 7, that is, for nonplanar $FeAu_n^+$ cluster substrates, and the excess charge on O_2 also is enhanced to 0.34 electrons for $n = 6$ and 0.32 (0.28) electrons for the isomer with $n = 7$ and multiplicity 5 (7).

To compare the adsorption properties of O_2 on cationic doped gold clusters with those for pure cationic gold clusters, it is convenient to relate the results for $(MAu_nO_2^+)_{ad}$ to those for $(Au_{n+1}O_2^+)_{ad}$ complexes displayed in Figures 1 and 6, respectively. The ratio of O_2 binding energy of $(MAu_nO_2^+)_{ad}$ to that of $(Au_{n+1}O_2^+)_{ad}$ is 5.8 (1.4), 4.3 (1.4), 6.7 (1.4), 9.3 (4.6), and 3.8 (1.2) for M = Ti (Fe) in the range of $n = 3-7$, respectively. The largest ratio in these series occurs for $n = 6$, just when the preferred M doped gold isomer becomes three dimensional, but the pure Au_7^+ cluster is still planar and has a minimum O_2 adsorption energy in the range studied here. Note that the $FeAu_7^+$ doped cluster has only a slightly larger O_2 highest adsorption energy than that of the pure Au_8^+ cationic cluster, the former leading to on top M and the latter to a bridge preferred adsorption site. Note also that the geometries of these $FeAu_7^+$ and Au_8^+ clusters are different. On the other hand, it was observed that the bridge Au-Au and on top M configurations of $(FeAu_4O_2^+)_{ad}$ have a similar adsorption energy, but the former has an analogous geometry to $(Au_5O_2^+)_{ad}$ in Figure 1. The comparison of O−O, as well as O−M versus O−Au, distances in $(MAu_nO_2^+)_{ad}$ and $(Au_{n+1}O_2^+)_{ad}$ represented in Figures 1 and 6, respectively, adds no further insight to the previous comments.

Dissociation Configurations of $MAu_nO_2^+$ Complexes. In the left part of Figure 7 are represented the minimum energy equilibrium configurations of $(MAu_nO_2^+)_{dis}$ complexes ($n = 3-7$ and M = Ti, Fe). These complexes were obtained by two procedures: (i) optimizing simultaneously the positions of two oxygen atoms attached to different sites of the lowest energy isomer of MAu_n^+ clusters as well as other MAu_n^+ isomers (which are represented in the first column of Figures 3–5) and (ii) an initially free O_2 molecule forced to have O−M and/or O−Au distances smaller than those found for $(MAu_nO_2^+)_{ad}$ complexes in equilibrium configurations. The formation energy of these $(MAu_nO_2^+)_{dis}$ complexes is calculated, similarly to eq 2, as

$$E_{dis}(n) = E[(MAu_n^+)_{GS}] + E[O_2] - E[(MAu_nO_2^+)_{dis}] \quad (5)$$

Here, $E_{dis}(n)$ is given, in eV, below each structure of Figure 7, together with the spin multiplicity (in parentheses). The most stable configuration for each size contains an O−M−O subunit with each O atom bonded to a different Au atom, and the geometry of the initial MAu_n^+ cluster becomes strongly deformed.

In the right upper panel of Figure 7 is represented the formation energy, $E_{dis}(n)$, which shows a similar behavior with size n and impurity M than $E_{ads}(n)$ of Figure 6, except that the odd−even effects for Fe complexes are lost at $n = 4$. Contrary to the complexes $(Au_{n+1}O_2^+)_{dis}$ discussed previously, the equilibrium configuration of $(MAu_nO_2^+)_{dis}$ with the highest formation energy is stable against the separation in MAu_n^+ and O_2 fragments. The maximum separation energy of $(MAu_nO_2^+)_{dis}$ is higher than the maximum O_2 adsorption energy of $(MAu_nO_2^+)_{ad}$ by a factor of 1.6 (2.5), 1.6 (1.7), 1.5 (2.4), 1.5 (1.3), and 1.6 (1.8) for M = Ti (Fe) and $n = 3-7$ complexes, respectively.

The behavior of the spin multiplicity of $(MAu_nO_2^+)_{dis}$ with respect to odd or even n complexes is similar to that for $(MAu_nO_2^+)_{ad}$ complexes. Note that the multiplicity of $(FeAu_7O_2^+)_{dis}$ is 6 instead of 7, which is an exception similar to that found for $(FeAu_7O_2^+)_{ad}$ in the previous subsection, and appears also for three dimensional $FeAu_n^+$ isomers. In the lower panel of Figure 7 is represented the second difference of the total energy, $E[(MAu_nO_2^+)_{dis}]$, which shows a peak at $n = 5$ for both Ti and Fe impurities of $(MAu_n^+O_2)_{dis}$ complexes.

To infer the roll of gold atoms in the tendencies shown in Figures 6 and 7 for $(MAu_nO_2^+)_{ad}$ and $(MAu_nO_2^+)_{dis}$, respectively, additional calculations for gas phase MO^+ and MO_2^+ molecules were performed. The lowest total energy state of the free TiO_2^+ (FeO_2^+) molecule forms an O−M−O angle ~90° (~113°), having a multiplicity of 2 (2) and M−O distance of 1.76 (1.65−1.69) Å. For the FeO_2^+ molecule, an isomeric state with ~0.6 eV higher total energy also was obtained, with a O−O−Fe angle of ~180°, Fe−O distance of 1.90 Å, and multiplicity of 8, which shows the strong interdependence of geometry and spin multiplicity. From Mulliken population analysis, the excess of nominal charge on O_2 for the ground state of TiO_2^+ (FeO_2^+) is 0.484 (0.203) electrons, and for the isomer of FeO_2^+ with a multiplicity of 8, it is 0.257 electrons. Similarly, the difference between spin-up and spin-down charge on O_2 (M) was 1.393 (−0.393) electrons for M = Ti and −0.380 (1.380) for M = Fe in the ground state. These numbers reflect the different sign of polarization induced on O_2 by Ti and Fe atoms. However, for FeO_2^+ with a multiplicity of 8, the difference between spin-up and spin-down charge on O_2 (Fe) was 3.085 (3.915) electrons, which illustrates the strong dependence of polarization on molecular geometry. For FeO^+, the preferred spin multiplicity was 6, Fe−O was 1.72 Å, and the excess electrons on O (Fe) was 0.26 (−1.26). A recent combined experimental and theoretical work[53] showed for FeO_2^+ that oxygen binds directly to Fe with no molecular O_2 units. In that work, the ground state of FeO_2^+ has a multiplicity of 2, Fe−O distance of 1.56 Å, angle O−Fe−O of ~115°, and (Mulliken) electron charge of 1.23 on Fe and 0.12 on each O. For diatomic FeO^+, a bond distance of 1.64 Å, multiplicity of 6, and excess electron charge of 0.20 (−1.20) electrons on O (Fe) were obtained. These values for FeO_2^+ and FeO^+ are similar to our results. Thus, it can be inferred that the role of gold atoms in maximum adsorption energy configurations of $(MAu_nO_2^+)_{dis}$ is to provide an environment for the coordination of M. We obtained that $(MAu_n^+O_2)_{dis}$ are stable against fragmentation in Au_n and MO_2^+, as well as Au_n^+ and MO_2 fragments.

Conclusion

A comparative theoretical study of the adsorption and dissociation of O_2 on pure Au_{n+1}^+ and doped Au_nM^+ (M = Ti, Fe) gold cationic clusters with $n = 3-7$ was performed. For pure Au_{n+1}^+ clusters, the O_2 molecule adsorbed preferably on top of the low coordinated Au atoms, except for Au_5^+ and Au_8^+ clusters, which prefer bridge adsorption sites. The geometry of Au_n^+ was preserved after O_2 adsorption. The adsorption energy on top of Au_n^+ was smaller than 0.5 eV, which is the limit for experimental observation[15,33] and decreased when the number of Au atoms increased. Instead, the adsorption energy in bridge positions of Au_n^+ was larger than 0.5 eV and was higher for $n = 8$ than for $n = 5$. The adsorption energy on cationic gold clusters is similar to that for neutral gold clusters but smaller than for anionic gold clusters obtained in previous works. Whereas the adsorption energy on Au_n^- anions is always higher

for top positions than for bridge positions, the opposite occurs for neutral Au_n with $n = 5$ and 7 and for cationic Au_n^+ with $n = 5$ and 8. The electronic charge flows towards O_2 when the molecule is adsorbed in bridge positions and towards the gold cluster when O_2 is adsorbed on top of Au atoms. The adsorption energy and O−O bond length of adsorbed oxygen increase when the amount of electronic charge on O_2 increases. Thus, for the bridge $(Au_8^+O_2)_{ad}$ complex, the distance Au−O is 2.16 Å (which is the minimum in the range of $n = 4-8$), and the distance of O−O is 1.34 Å (which is the maximum in the range of $n = 4-8$), corresponding to a superoxo state of adsorbed O_2.

On the other hand, the highest adsorption energy of $(MAu_nO_2^+)_{ads}$ was obtained when both atoms of O_2 bind on top of the M impurity in the ground state of the MAu_n^+ clusters. For $n = 6$, $FeAu_7^+$ prefers the on top M site of other (nonplanar) isomers. The highest adsorption energy is larger for Ti doped clusters than for those doped with Fe by factors of 4.0, 3.2, 4.9, 2.0, and 3.2 for $n = 3$, 4, 5, 6, and 7, respectively, and shows an odd−even effect trend with size n, which is opposite for Ti as compared to Fe complexes. The adsorption energy is higher also for Ti complexes in the second preferred configuration, namely, the bridge M-Au type. That configuration competes with the bridge Au-Au and on top Au types for M = Fe and $n = 4-6$. The highest adsorption energy of $(MAu_nO_2^+)_{ad}$ is higher than that for $(Au_{n+1}O_2^+)_{ad}$ by a factor of ∼4.0 (1.2) for M = Ti (M = Fe). However, for the on top Au and bridge Au-Au equilibrium configurations of $(MAu_nO_2^+)_{ad}$, the adsorption energy is similar to or smaller than similar configurations of $Au_{n+1}O_2^+$ complexes. The trends for $(Au_nO_2^+)_{ad}$ and $(MAu_nO_2^+)_{ad}$ complexes can be rationalized in terms of the O−O and O−M bond distances, as well as the charge transfer among oxygen and cluster substrates. From Mulliken population analysis, it is concluded that the larger the excess of electron charge on O_2 is, the highest (smaller) the adsorption energy (O−M bond distance) is. The O−O bond distance is larger than 1.30 (1.43) Å for $(MAu_nO_2^+)_{ad}$ complexes with M = Fe (M = Ti), which is that adsorbed O_2 presents a superoxo state able to react with radicals such as CO. However, for $(Au_nO_2^+)_{ad}$, the O−O distance is larger than 1.30 only for $n = 8$.

It is interesting to note that doped MAu_n^+ clusters are good candidates for coadsorption of CO and O_2 and subsequent CO oxidation because CO prefers to bind the less coordinated apex atoms of gold cluster cations (see Figure 5 in ref 18), whereas O_2 prefers to bind the M impurity, which is always highly coordinated in the doped MAu_n^+ cluster. For example, CO probably forms a O−C−Au bond with the Au atom closest to the M impurity of $(MAu_7O_2^+)_{ad}$ complexes shown in Figure 5. Furthermore, because O_2 in these complexes has an enhanced O−O distance, it easily forms a metastable peroxide-like intermediate state O−O−C−O leading to a final state with a desorbed CO_2 molecule and an adsorbed O atom on the cluster. To substantiate this qualitative description, we will perform further calculations.

An interesting result of this work is that the spin multiplicity of those $(MAu_nO_2^+)_{ad}$ complexes with the highest O_2 adsorption energy is a maximum (minimum) for M = Fe (Ti), corresponding to parallel (anti-parallel) spin coupling of MAu_n^+ clusters and O_2 molecules. That different coupling leads to odd−even alternation of the spin multiplicity, which is opposite for Ti and Fe complexes. That odd−even effect is opposite to the odd−even effect of the corresponding adsorption energies (see Figure 6).

The minimum energy equilibrium structure of $(Au_nO_2^+)_{dis}$ and $(MAu_nO_2^+)_{dis}$ containing two separated O atoms bonded at different sites of Au_n^+ and MAu_n^+ clusters, respectively, also were computed. The initial ground-state geometries of Au_n^+ and MAu_n^+ clusters strongly were deformed. For $(MAu_nO_2^+)_{dis}$, the configuration with the highest adsorption energy contained the unit O−M−O and was stable against the separation in the ground states of MAu_n^+ and O_2 fragments, respectively. Instead, for $(Au_nO_2^+)_{dis}$, only complex $n = 6$ is stable against the separation in Au_n^+ and O_2 fragments. The maximum separation energy of $(MAu_nO_2^+)_{dis}$ is higher than the O_2 adsorption energy of $(Au_{n+1}O_2^+)_{ad}$ complexes by a factor of ∼1.6 (2.5), 1.6 (1.7), 1.5 (2.4), 1.5 (1.3), and 1.6 (1.8) for M = Ti (Fe) complexes in the range of $n = 3-7$, respectively. These ratios indicate that doped MAu_n^+ clusters prefer to dissociate O_2 than to adsorb O_2, particularly those gold cationic clusters with an iron atom impurity.

Acknowledgment. We acknowledge financial support from the Spanish IFCTY under the FEDER organization of the European Community (Grant Mat2005-03415) and Junta de Castilla y León (Grant VA-068A06). The Centre for Atomic-Scale Material Design is funded by the Lundbeck Foundation. E.M.F. acknowledges support from the Danish Research Agency (Grant 26-04-007) and the Danish Centre for Scientific Computing (Grant HDW-0107-07).

References and Notes

(1) Zhai, H.-J.; Wang, L.-S. *J. Chem. Phys.* **2005**, *122*, 51101.
(2) Xu, Q.; Jiang, L. *J. Phys. Chem. A* **2006**, *110*, 2655.
(3) Haruta, M. *Catal. Today* **1997**, *36*, 153.
(4) Cox, D. M.; Brickman, R.; Creegan, K.; Kaldor, A.Z. *Z. Phys. D* **1991**, *19*, 353.
(5) (a) Wallace, W. T.; Wheten, R. L. *J. Am. Chem. Soc.* **2002**, *124*, 7499. (b) Wallace, W. T.; Wyrwas, R. B.; Wheten, R. L.; Mitric, R.; Bonacic-Koutecký, V. *J. Am. Chem. Soc.* **2003**, *125*, 8408.
(6) (a) Hagen, J.; Socaciu, L. D.; Elijazyfer, M.; Heiz, U.; Bernhardt, T. M.; Wöste, L. *Phys. Chem. Chem. Phys.* **2002**, *4*, 1707. (b) Socaciu, L. D.; Hagen, J.; Bernhardt, T. M.; Wöste, L.; Heiz, U.; Häkkinen, H.; Landman, U. *J. Am. Chem. Soc.* **2003**, *125*, 10437.
(7) (a) Yoon, B.; Häkkinen, H.; Landman, U. *J. Phys. Chem. A* **2003**, *107*, 4066. (b) Yoon, B.; Koskinen, P.; Huber, B.; Kostko, O.; von Issendorff, B.; Häkkinen, H.; Moseler, M.; Landman, U. *Chem. Phys. Chem.* **2007**, *8*, 157.
(8) Franceschetti, A.; Pennycook, S. J.; Pantelides, S. T. *Chem. Phys. Lett.* **2003**, *374*, 471.
(9) Fernández, E. M.; Torres, M. B.; Balbás, L. C. Recent advances in the theory of chemical and physical systems. In *Progress in Theoretical Chemistry and Physics*, 15th ed.; Julien, J. P., Maruani, J., Mayou, D., Wilson, S., Delgado-Barrio, G., Eds.; Springer: Berlin, 2006; p 407.
(10) Yuan, D. W.; Zeng, Z. *J. Chem. Phys.* **2004**, *120*, 6574.
(11) Luo, C.; Fa, W.; Dong, J. *J. Chem. Phys.* **2006**, *125*, 84707.
(12) Fernández, E. M.; Ordejón, P.; Balbás, L. C. *Chem. Phys. Lett.* **2005**, *408*, 252.
(13) Barton, D. G.; Podkolzin, S. J. *Phys. Chem. B* **2005**, *109*, 2262.
(14) Barrio, L.; Liu, P.; Rodriguez, J. A.; Campos-Martin, J. M.; Fierro, J. L. G. *J. Phys. Chem. C* **2007**, *111*, 19001.
(15) Ding, X.; Li, Z.; Yang, J.; Hou, J. G.; Zhu, Q. *J. Chem. Phys.* **2004**, *120*, 9594.
(16) Prestianni, A.; Martorana, A.; Labat, F.; Ciofini, I.; Adamo, C. *J. Phys. Chem. B* **2006**, *110*, 12240.
(17) Joshi, A. M.; Delgass, W. N.; Thomson, K. *J. Phys. Chem. B* **2005**, *109*, 22392.
(18) Neumaier, M.; Weigend, F.; Hampe, O.; Kappes, M. M. *Faraday Discuss.* **2008**, *138*, 393.
(19) Häkkinen, H.; Abbet, S.; Sanchez, A.; Heiz, U.; Landman, U. *Angew. Chem., Int. Ed.* **2003**, *42*, 1297.
(20) Tielens, F.; Andrés, J.; Van Brussel, M.; Buess-Hermann, C.; Geerlings, P. *J. Phys. Chem. B* **2005**, *109*, 7624.
(21) Furche, F.; Ahlrichs, R.; Weis, P.; Jacob, C.; Gilb, S.; Bierweiler, T.; Kappes, M. M. *J. Chem. Phys.* **2002**, *117*, 6982.
(22) Lee, H. M.; Ge, M.; Sahu, B. R.; Tarakeshwar, P.; Kim, K. S. *J. Phys. Chem. B* **2003**, *107*, 9994.
(23) Häkkinen, H.; Yoon, B.; Landman, U.; Li, X.; Zhai, H.-J.; Wang, L.-S. *J. Phys. Chem. A* **2003**, *107*, 6168.
(24) Fernández, E. M.; Soler, J. M.; Garzón, I. L.; Balbás, L. C. *Phys. Rev. B: Condens. Matter Mater. Phys.* **2004**, *70*, 165403.

(25) Gilb, S.; Weis, P.; Furche, F.; Ahlrichs, R.; Kappes, M. M. *J. Chem. Phys.* **2002**, *116*, 4094.
(26) Torres, M. B.; Fernández, E. M.; Balbás, L. C. *Phys. Rev. B: Condens. Matter Mater. Phys.* **2005**, *71*, 155412.
(27) (a) Neukermans, S.; Janssens, E.; Tanaka, H.; Silverans, R. E.; Lievens, P. *Phys. Rev. Lett.* **2003**, *90*, 33401. (b) Janssens, E.; Tanaka, H.; Neukermans, S.; Silverans, R. E.; Lievens, P. *Phys. Rev. B: Condens. Matter Mater. Phys.* **2004**, *138*, 393.
(28) (a) Pyykko, P.; Runeberg, N. *Angew. Chem., Int. Ed.* **2002**, *41*, 2174. (b) Li, X.; Kiran, B.; Li, J.; Zhai, H.-J.; Wang, L.-S. *Angew. Chem., Int. Ed.* **2002**, *41*, 4786. (c) Zhai, H.-J.; Wang, L.-S. *J. Chem. Phys.* **2004**, *121*, 8369.
(29) (a) Graciani, J.; Oviedo, J.; Sanz, J. F. *J. Phys. Chem. B* **2006**, *110*, 11600. (b) Yuan, D. W.; Wang, Y.; Zeng, Z. *J. Chem. Phys.* **2005**, *122*, 114310.
(30) Jacob, T.; Merinov, B. V.; Goddad, W. A., III *Chem. Phys. Lett.* **2004**, *385*, 374.
(31) Florez, E.; Mondragón, F.; Fuentealba, P. *J. Phys. Chem. B* **2006**, *110*, 13793.
(32) Kim, Y. D.; Ganteför, G. *Chem. Phys. Lett.* **2003**, *382*, 644.
(33) Ghanty, T. K. *J. Chem. Phys.* **2005**, *123*, 241101.
(34) (a) Fu, L.; Wu, N. Q.; Yang, J. H.; Qu, F.; Johnson, D. L.; Kung, M. C.; Kung, H. H.; Dravid, V. P. *J. Phys. Chem. B* **2005**, *109*, 3704. (b) Stiehl, D. J.; Kim, T. S.; McClure, S. M.; Mullins, C. B. *J. Am. Chem. Soc.* **2004**, *126*, 13574. (c) Lee, S.; Fan, C.; Wu, T.; Anderson, S. L. *J. Am. Chem. Soc.* **2004**, *126*, 5682. (d) Molina, L. M.; Hammer, B. *Appl. Catal., A* **2005**, *291*, 21. (e) Meerson, O.; Sitja, G.; Henry, C. R. *Eur. Phys. J. D* **2005**, *34*, 119. (f) Broqvist, P.; Molina, L. M.; Grömbeck, H.; Hammer, B. *J. Catal.* **2004**, *227*, 217.
(35) Zhai, H.-J.; Wang, L-S. *J. Chem. Phys.* **2005**, *122*, 51101.
(36) Wallace, W. T.; Leawitt, A. J.; Wetten, R. L. *Chem. Phys. Lett.* **2003**, *368*, 774.
(37) Laureen, S.; Linic, S. *Phys. Rev. Lett.* **2006**, *97*, 26101.
(38) Molina, L.; Hammer, B. *Phys. Rev. B: Condens. Matter Mater. Phys.* **2004**, *69*, 155424.
(39) Guzman, J.; Gates, B. C. *J. Am. Chem. Soc* **2004**, *126*, 26722.
(40) Chrètien, S.; Metiu, H. *J. Chem. Phys.* **2007**, *126*, 104701.
(41) Weiher, N.; Beesley, A. M.; Tsapatsaris, N.; Delannoy, L.; Louis, C.; van Bokhoven, J. A.; Schroeder, S. L. M. *J. Am. Chem. Soc.* **2007**, *129*, 2240.
(42) Kung, M. C.; Davis, R. J.; Kung, H. H. *J. Phys. Chem.* **2007**, *111*, 11767.
(43) Bond, C. C.; Thompson, D. T. *Gold Bull.* **2000**, *33*, 41.
(44) Guzman, J.; Gates, B. C. *J. Phys. Chem. B* **2002**, *106*, 7659.
(45) Salama, T. M.; Ohnishi, R.; Shido, T.; Ichikawa, M. *J. Catal.* **1995**, *152*, 169.
(46) Finch, R. M.; Hodge, N. A.; Hutchings, G. J.; Meagher, A.; Pankhurst, Q. A.; Siddiqui, M. R. H.; Wagner, F. E.; Whyman, R. *Phys. Chem. Chem. Phys.* **1999**, *1*, 485.
(47) Meyer, R.; Lemire, C.; Shaikhutdinov, S. K.; Freund, H.-J. *Gold Bull.* **2004**, *37*, 72.
(48) Soler, J. M.; Artacho, E.; Gale, J. D.; García, A.; Junquera, J.; Ordejón, P.; Sánchez-Portal, D. *J. Phys: Condens. Matter* **2002**, *14*, 2745.
(49) Perdew, J. P.; Burke, K.; Ernzerhof, M. *Phys. Rev. Lett.* **1996**, *77*, 3865.
(50) Troullier, M.; Martins, J. L. *Phys. Rev. B: Condens. Matter Mater. Phys.* **1991**, *43*, 1993.
(51) Fonseca-Guerra, C.; Handgraaf, J.-W.; Baerends, E. J.; Bickelhaupt, F. M. *J. Comput. Chem.* **2003**, *25*, 189.
(52) Tielens, F.; Gracia, L.; Polo, V.; Andrés, J. P. *J. Phys. Chem. A* **2007**, *111*, 13255.
(53) Reilly, N. M.; Reveles, J. U.; Johnson, G. E.; Campo, J. M.; Khana, S. N.; Köster, A. M.; Castleman, A. W., Jr *J. Phys. Chem. A* **2007**, *111*, 4158.

JP800247N